$\mathcal{AIPS}$ Memo 125
Post-Correlation Basis Conversion in $\mathcal{AIPS}$

Rick Perley and Eric Greisen
National Radio Astronomy Observatory, Socorro, NM

April 16, 2024

Abstract

Calibration and imaging of interferometric visibility data are much simpler when the receiver systems are designed to provide output voltages proportional to the circular components of the electric field. On the other hand, the antenna performance (sensitivity, and polarization purity over wide bandwidths) is much better for data taken with linear-basis receivers. In this memo, we describe how post-correlation visibility data can be converted from its original linear basis to a circular basis. Doing so enables better calibration and imaging while maximizing sensitivity and polarization purity. Examples are given using VLA and MeerKAT data. [1]

1 Motivation

Polarimetry requires antennas which are themselves polarized – each producing two output signals representing two different polarization states. In principle, it doesn't matter what these two polarization states are, so long as they are different. In practice, the processes of calibration and imaging are simplified if the two states are orthogonal[2] – usually either opposite circular (RCP and LCP) or orthogonal linear (for example, vertical and horizontal).

Thus, engineers design the receiver systems (antennas, receivers, amplifiers, and signal transmission) such that the two output voltages provided to the correlator represent, as closely as possible, either the opposite circular electric field components of the incoming radiation, or the orthogonal linear components. If done well, subsequent calibration is straightforward, and the imaging results will be the same – all else being equal.

But all else is *not* equal. Linear basis data are usually more difficult to accurately calibrate, since virtually all calibrator sources used in the meter-to-millimeter wavelength range are significantly ($\sim$2 – 10%) linearly polarized. This linearly polarized flux couples directly with the linear feeds, causing the output correlations to vary sinusoidally with parallactic angle – a situation which can be easily handled if the polarization state is known in advance. Unfortunately, the great majority of these calibrator sources are variable, both in total intensity and in fractional polarization, on timescales varying from days to months, with amplitudes of a few to tens of percent. Monitoring the flux density and polarization characteristics of the more than 1000 VLA calibrators on such timescales with the VLA's eight receiver bands is simply not feasible. Thus, the polarization state of the calibrators used in any observation will not, in general, be known in advance[3]. Furthermore, at low frequencies ($<\sim$3 GHz), the ionosphere dynamically rotates the observed plane of polarization on timescales of seconds to hours, thus requiring estimation of the ionospheric Faraday rotation measure (IFRM) – a significant complicating factor.

These calibration complications are avoided if the data are taken in a circular basis, for which the knowledge of the linear polarization state of the calibrators is not needed for gain calibration, as the linear polarized state of the radiation is entirely encoded in the cross-hand correlations. And while the circular component of the source radiation is directly coupled to circular feeds, the fractional circularly polarized flux, V/I, is always less than 1% for calibrator sources, and can be safely ignored in standard gain calibration.

Unfortunately, producing wide-band dual-polarization signals accurately proportional to the electric field's circular components is technically difficult. To our knowledge, all modern wide-band receiver systems utilized in astronomy natively produce output voltages proportional to the linear components of the electric field. To obtain the desired

[1] This memo has also appeared as EVLA Memo 229.

[2] In this context, orthogonal means the antenna's two polarization states are oppositely directed in the Poincaré sphere.

[3] For observations taken over a considerable length of time, the polarization states of the calibrators can be determined from the data. However, this cannot be done for short-duration observations, an increasingly common mode of observation.

circular-basis voltages, an additional device which provides the appropriate 90 degree phase shifts and signal combinations must be added to the receiver system. These devices are not perfect – they add noise, and are difficult (or impossible) to design for good performance over very wide bandwidths. Thus, while there are strong reasons to prefer a circular basis for calibration and imaging, there are also strong engineering arguments for remaining in the linear basis.

It is important to emphasize that these statements also hold true for self-calibration – a critical calibration step needed for high-fidelity imaging. With linear systems, the self-calibration operation will in general require source models in three Stokes parameters (I, Q, and U), while for circular systems, only a Stokes I model is required. We reemphasize also that at low frequencies, ionospheric effects rotate the incoming plane of polarization on timescales of seconds to hours. For linear systems, these rotations must be accounted for in both standard and self-calibration operations, while for circular systems, these rotations can be ignored[4].

We illustrate these points in the next section.

2 Interferometric Response to Polarized Radiation

Astronomers use the Stokes parameters[5] (I, Q, U, and V) to describe the polarization state of electromagnetic radiation. They are real numbers, which greatly facilitate their use in visual presentations for resolved sources.

The correlations provided by an interferometer are functions of the two antennas' polarization states and the source polarization state. The most general expression relating these correlations to the antennas and source polarizations was published in 1963 by Morris, Radakrishnan, and Seielstad[6]. The relationship can be written as:

$$\begin{aligned} R_{mn} &= G_{mn}\{[\cos(\chi_m-\chi_n)-\sin(\chi_m+\chi_n)]e^{-i\Delta\Psi}(\mathcal{I}+\mathcal{V})/4 \\ &\quad +[\cos(\chi_m+\chi_n)-\sin(\chi_m-\chi_n)]e^{-i\Sigma\Psi}(\mathcal{Q}+i\mathcal{U})/4 \\ &\quad +[\cos(\chi_m+\chi_n)+\sin(\chi_m-\chi_n)]e^{i\Sigma\Psi}(\mathcal{Q}-i\mathcal{U})/4 \\ &\quad +[\cos(\chi_m-\chi_n)+\sin(\chi_m+\chi_n)]e^{i\Delta\Psi}(\mathcal{I}-\mathcal{V})/4\} \end{aligned} \quad (1)$$

where $\mathcal{I},\mathcal{Q},\mathcal{U}$, and $\mathcal{V}$ are the Stokes visibilities of the source structure in Stokes I, Q, U, and V, χ_m is the antenna ellipticity for signal channel m, $\Sigma\Psi=\Psi_m+\Psi_n$ and $\Delta\Psi=\Psi_m-\Psi_n$ are the sum and difference of the two antennas' ellipticity position angles for the correlation pair under consideration. Note that the antenna ellipticity position angle, Ψ, is in sky coordinates, so will in general include both the antenna ellipticity angle ψ, measured in the antenna coordinate frame, and the antenna parallactic angle, Ψ_p. G_{mn} is a correlator-based gain for the pair under consideration, and is normally factored into a product of the two component antennas' gains: $G_{mn}=G_mG_n^*$.

This rather fearsome expression produces very simple results when pure linear and pure circular basis antennas are considered.

2.1 Pure Circular

In this case, the antenna ellipticities for the right and left polarizations are $\chi_r=-\pi/4$, and $\chi_l=\pi/4$, so the visibilities become:

$$R_{rr} = G_{r1}G_{r2}^*(\mathcal{I}+\mathcal{V})/2 \quad (2)$$
$$R_{rl} = G_{r1}G_{l2}^*e^{-i2\Psi_p}(\mathcal{Q}+i\mathcal{U})/2 \quad (3)$$
$$R_{lr} = G_{l1}G_{r2}^*e^{i2\Psi_p}(\mathcal{Q}-i\mathcal{U})/2 \quad (4)$$
$$R_{ll} = G_{l1}G_{l2}^*(\mathcal{I}-\mathcal{V})/2 \quad (5)$$

where Ψ_p is the antenna parallactic angle, a known quantity, and which for simplicity we have assumed is the same for the two antennas (a condition which is very close to true for the VLA and MeerKAT)[7].

Note that the parallel-hand responses are solely functions of Stokes $\mathcal{I}$ and $\mathcal{V}$, while the cross-hand responses are solely functions of Stokes $\mathcal{Q}$ and $\mathcal{U}$. Since the fractional circular polarization V/I is less than 1% for all calibrator sources, we can usually ignore the $\mathcal{V}$ visibility for the purposes of calibration, thus simplifying the process of gain

[4] Of course, for polarimetric imaging, the ionospheric rotations must be accounted for in both systems.
[5] Originally defined by George Stokes in 1852 for use in optics, and extended to astronomy by Chandrasekhar in 1946.
[6] Ap.J. **139**, 551, 1963
[7] The antenna ellipticity angle dependence is absorbed into the gain phase factors.

calibration, which then needs to know only the value of $\mathcal{I}$, which for a point source at the phase center is a real number, equal to the flux density.

From Equations 2 – 5, the Stokes visibilities are found to be:

$$\begin{aligned}
\mathcal{I} &= R'_{rr} + R'_{ll} && (6)\\
\mathcal{V} &= R'_{rr} - R'_{ll} && (7)\\
\mathcal{Q} &= e^{-i2\Psi_p} R'_{rl} + e^{i2\Psi_p} R'_{lr} && (8)\\
i\mathcal{U} &= e^{i2\Psi_p} R'_{rl} - e^{-i2\Psi_p} R'_{lr} && (9)
\end{aligned}$$

where the prime indicates calibrated visibilities. The $\mathcal{I}$ and $\mathcal{V}$ visibilities utilize only the parallel-hand correlations, while the $\mathcal{Q}$ and $\mathcal{U}$ visibilities utilize only the cross-hand correlations.

Contrast this simple situation to that for pure linear systems, shown next.

2.2 Pure Linear

In this case, the antenna ellipticities are zero: $\chi = 0$, and the antenna polarization ellipse position angles are aligned with the dipole feeds, and are orthogonal. Thus: $\Psi_v = \Psi_p, \Psi_h = \Psi_p + \pi/2$, where we are assuming the antennas have az-el mounts. Equation 1 then gives:

$$\begin{aligned}
R_{vv} &= G_{v1}G^*_{v2}[\mathcal{I} + \mathcal{Q}\cos(2\Psi_p) + \mathcal{U}\sin(2\Psi_p)]/2 && (10)\\
R_{vh} &= G_{v1}G^*_{h2}[-\mathcal{Q}\sin(2\Psi_p) + \mathcal{U}\cos(2\Psi_p) + i\mathcal{V}]/2 && (11)\\
R_{hv} &= G_{h1}G^*_{v2}[-\mathcal{Q}\sin(2\Psi_p) + \mathcal{U}\cos(2\Psi_p) - i\mathcal{V}]/2 && (12)\\
R_{hh} &= G_{h1}G^*_{h2}[\mathcal{I} - \mathcal{Q}\cos(2\Psi_p) - \mathcal{U}\sin(2\Psi_p)]/2 && (13)
\end{aligned}$$

again assuming the antennas' parallactic angles are the same and the antenna feeds are correctly aligned[8].

All four correlations are now functions of three Stokes' visibilities. In particular, both linear visibilities $\mathcal{Q}$ and $\mathcal{U}$ are involved in the two parallel-hand correlations. Gain calibration using these high-signal correlations thus requires knowledge of the source Q and U flux values – which are not usually known in advance.

These equations give solutions:

$$\begin{aligned}
\mathcal{I} &= R'_{vv} + R'_{hh} && (14)\\
i\mathcal{V} &= R'_{vh} - R'_{hv} && (15)\\
\mathcal{Q} &= (R'_{vv} - R'_{hh})\cos(2\Psi_p) - (R'_{vh} + R'_{hv})\sin(2\Psi_p) && (16)\\
\mathcal{U} &= (R'_{vv} - R'_{hh})\sin(2\Psi_p) + (R'_{vh} + R'_{hv})\cos(2\Psi_p) && (17)
\end{aligned}$$

In contrast to the pure circular case, all four correlations are in general required to derive the $\mathcal{Q}$ and $\mathcal{U}$ Stokes visibilities.

3 Post-Correlation Basis Conversion

We noted in the introduction that there are strong engineering reasons to utilize linear-basis antennas, due to superior sensitivity, bandwidth, and polarization purity. However, for the processes of calibration and self-calibration, circular-basis signals are much preferred. Can we have both? Is it possible to convert the linear-based visibilities provided by an interferometer to circular-based visibilites? The answer – happily – is yes, and is useful to do so, provided certain conditions are met.

It is useful to first consider how modern receiver systems generate outputs proportional to circular polarization. To do this, the voltage from the horizontal dipole is advanced (phase shifted) by 90 degrees, then added to the vertical dipole signal, creating a voltage proportional to the right-circular voltage component. Similarly, to generate the left-circular component, the horizontal voltage must be delayed (phase retarded) by 90 degrees, then added to the vertical dipole signal. The necessary 90-degree phase shifts must be the same across the full bandwidth of the receiver, and the input signal amplitudes must be balanced. For the JVLA, at L, S, and C bands, a microwave coaxial hybrid coupler, following the OMT, does the combining. These devices are remarkably wideband – a 2:1 BWR – but are also rather poorly balanced, producing output voltages with significant frequency-dependent ellipticity. At

[8]Inclusion of these offsets is straightforward, but needlessly complicates the equations, and obfuscates the central points.

X, Ku, K and Ka bands, a corrugated phase-shifter combined with a 45-degree rotation transition before the OMT is employed. These provide better performance than the coaxial couplers, but have a narrower BWR – 1.5:1. At Q-band, a waveguide septum polarizer providing native circularly polarized outputs is used (and are utilized at all bands on the VLBA). This is a much simpler and highly compact device, but of much narrower BWR – 1.2:1.

In terms of the analytic signals V_v and V_h, corresponding to the linear-basis components of the astronomical signal as measured by an alt-az antenna, the operations described above are given by a simple matrix equation $V_{cir} = JV_{lin}$:

$$\begin{pmatrix} V_r \\ V_l \end{pmatrix} = \begin{pmatrix} 1 & i \\ 1 & -i \end{pmatrix} \begin{pmatrix} V_v \\ V_h \end{pmatrix} \tag{18}$$

where the 2 x 2 coupling matrix J is known as the Jones matrix, and the column voltage vectors V_{cir} and V_{lin} are the antenna responses for the circular and linear bases.

These simple equations hide an important caveat: For the conversion to be useful, the amplitudes of V_v and V_h must be accurately balanced, so that their ratio for an unpolarized source is near unity, and the phase difference between them must be close to zero. The desired accuracy and stability of these limits will be discussed later.

We represent the four correlations derived from a single baseline by a column vector R, each element being defined by a complex multiplication – for example, $R_{rr} = V_{r1}V^*_{r2}$. The relation between the output circular-basis vector R_c and the input linear-basis vector R_l is found from the outer product of the two antennas' Jones matrices: $R = J_1 \otimes J_2^*$, giving:

$$\begin{pmatrix} R_{rr} \\ R_{rl} \\ R_{lr} \\ R_{ll} \end{pmatrix} = \begin{pmatrix} 1 & -i & i & 1 \\ 1 & i & i & -1 \\ 1 & -i & -i & -1 \\ 1 & i & -i & 1 \end{pmatrix} \begin{pmatrix} R_{vv} \\ R_{vh} \\ R_{hv} \\ R_{hh} \end{pmatrix} \tag{19}$$

It is of course possible to execute the inverse operation – converting a circular-basis dataset into the linear-basis. For completeness, we give the inverse transform (ignoring scaling factors):

$$\begin{pmatrix} R_{vv} \\ R_{vh} \\ R_{hv} \\ R_{hh} \end{pmatrix} = \begin{pmatrix} 1 & 1 & 1 & 1 \\ i & -i & i & -i \\ -i & -i & i & i \\ 1 & -1 & -1 & 1 \end{pmatrix} \begin{pmatrix} R_{rr} \\ R_{rl} \\ R_{lr} \\ R_{ll} \end{pmatrix} \tag{20}$$

3.1 Implementation into *AIPS*

The basis conversions defined above have been implemented in the *AIPS* task `VH2RL`, and the results (from linear to circular) tested using both VLA P band data, and MeerKAT UHF band data.

As noted above, it is important that good amplitude and phase matching of the linear-basis data be obtained before combination. In practical terms, this means that a pure linear input signal gives the same output amplitude and phase when observed oriented with the vertical and horizontal dipoles, or, equivalently, observation of an unpolarized source provides the same output amplitudes in both signal channels. Similarly, the signal phase paths, from sky to correlator, must be the same for both polarization channels. Combination of the signals with deviations from these conditions will result in an elliptically polarized signal, which will show up as D terms in the calibration. These conditions are the same as those imposed on analog conversion of the voltage signals done at the antenna. These points are further developed in Section 5.

4 Examples Using VLA and MeerKAT Data

Here we show some examples, using data taken with these two arrays, focusing on the calibration steps required to ensure proper amplitude and phase matching prior to basis conversion.

4.1 A VLA P-band Observation

We show results from C-configuration data taken 13Dec2022 with the VLA's linearly-polarized P-band system, as part of a lunar polarimetry experiment. At these low frequencies, there are very few sources with high linearly-polarized emission, and only four for which we know the intrinsic polarization properties[9]. These are the Moon, the

[9]The details of our determination of these properties will be given in a following EVLA Memo.

compact and bright hotspots of DA240 and 3C303, and the quasar 3C345[10].

The VLA's P-band system nominally covers a 256 MHz-wide span of frequencies, from 224 to 480 MHz. Due to RFI, only half of this can be usefully employed for science observations when the array is in the D and C configurations. For the lunar polarization program data utilized here, we retained two 64-MHz-wide bands which are relatively free of RFI: the lower one spanning 288 – 352 MHz, the upper spanning 384 – 448 MHz. For each of these blocks, the correlator was configured to provide the data in four spectral windows, each 16 MHz wide, with 1-second averaging and 125 kHz spectral resolution. The results shown here are from the lower band.

The goal of this program was to provide data for improving our calibration procedures for low-frequency polarimetric observations. The target object observed was the Moon, whose polarization properties are exactly known, but which is also heavily resolved and of low surface brightness, so cannot serve as any sort of calibrator. The primary gain calibration sources observed were 3C147 and 3C295, both of which are very strong (over 50 Jy) and unpolarized. Additionally, the polarized sources DA240 (whose northern hotspot is nearly 20% polarized) and the unresolved quasar 3C345, (whose nucleus is polarized at about the 2 – 4 % level), and a nearby amplitude and phase calibrator, J1021+2159, whose polarization state was unknown, were included.

To enable successful conversion of the linear-basis visibilities to a circular basis, the parallel-hand gains must be equalized, and any phase offset between the two channels removed. For the VLA, no attempt is made to ensure these requirements are met via gain and phase adjustments to the on-line systems, so they must be done post-correlation to the linear-basis visibility data.

In what follows, we describe the minimal pre-conversion calibration process. The two essential operations are to equalize the antenna gains of the two polarization channels, and to remove any phase difference between them. Both operations must be done as a function of frequency, as spectral variations in amplitude and phase are ubiquitous in these systems.

Following flagging to remove non-functional antennas and RFI contamination, the data were decimated by a factor of 80 (10 in time, and 8 in frequency), to 10-seconds and 1 MHz to facilitate calibration and imaging. We then performed the following operations:

1. `BPASS`. This program solves for the spectral variations in antenna amplitude and phase. For the purpose of gain balancing, the flux density of the calibrator source is not needed – we chose the default 1 Jy – but it is critical that the calibrator source chosen be unpolarized. For simplicity, we utilized a single scan of 3C147. Because our goal is to balance the V and H gains, and we did not utilize the gain calibration program `CALIB`, the `BPASS` program must be used in its absolute mode – no normalization of the resulting spectral amplitude solutions. The phase solutions are with respect to the reference antenna, and will include the parallel-hand delays.

   Example solutions for three antennas are shown in the left hand panel of Fig. 1. The amplitude solutions show the characteristic drop-outs due to the attenuation at the edges of the four spectral windows. The slopes in the phase solutions are due to differential delays between the the target and reference antenna, and are different for the two polarization channels. Application of the bandpass solutions removes spectral amplitude and phase variations for each polarization channel, leaving only the spectral phase differences between the two polarization channels of the reference antenna. These are removed by the following two programs.

2. `RLDLY`. The delay removal included in the `BPASS` operation is not sensitive to the delays between the two polarization channels, which will appear as a phase slope in the cross-hand phase spectra. Due to this, it proves generally necessary to utilize `RLDLY` to find and remove this delay. In principle, a polarized source should be used, but in practice, due to the small but significant misorientations of the dipoles, a strong unpolarized source serves as well. We used the unpolarized source 3C147 for this determination. The resulting delay was 3.7 nsec, corresponding to a phase slope of 85 degrees over the 64 MHz total bandwidth.

3. `VHDIF`. This program removes the residual cross-hand (V-H) phase of the reference antenna. This phase is calculated from the expression $\tan\phi = -V/U$, so requires the observation of a strongly polarized compact source[11]. We used the eastern hotspot of DA240, which provides nearly 500 mJy of polarized flux. The position angle of the polarized signal does not need to be known for this operation. However, two solutions, differing by

[10]The planets Mars and Venus have known polarization properties, but are too small and weak to be used by the VLA at these low frequencies.

[11]The curious reader might wonder why `VHDIF` cannot also remove the cross-hand delay, thus bypassing the need for `RLDLY`. The answer is that `VHDIF` can, but gets into trouble when the absolute value of the cross-hand phase is close to 90 degrees, since the value of $\mathcal{U}$ is then close to zero. A large delay value greatly increases the chance that some channels will be close to this condition. If, by bad luck, the cross-hand phase for all channels is close to 90 degrees following `RLDLY`, one must insert with `CLCOR` an offset phase to the H channel, to enable `VHDIF` to find a good solution.

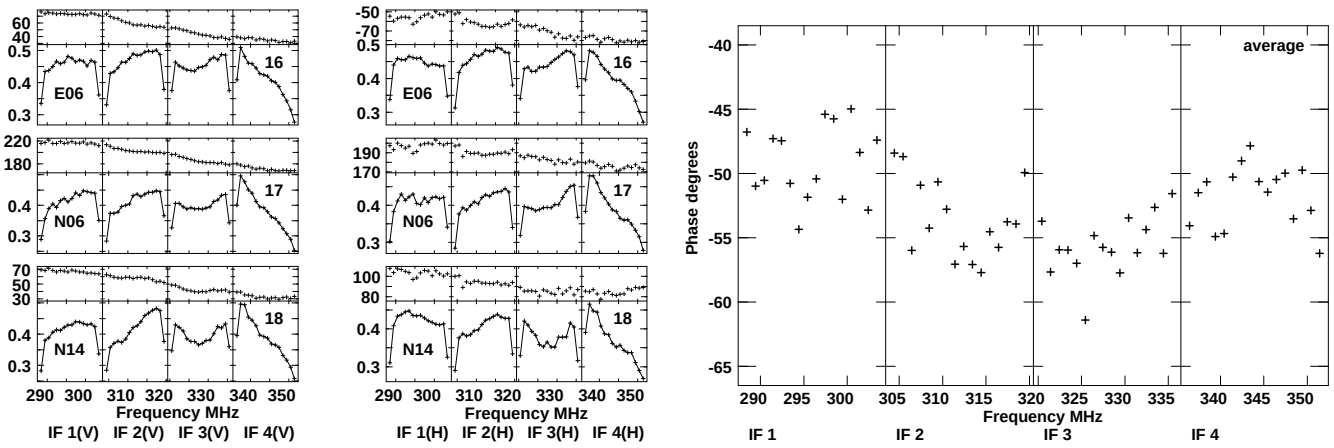

Figure 1: **Left Panel:** Showing the absolute bandpass solutions from 3C147, assuming unit flux density, for antennas ea16, ea17, and ea18. The left column shows the vertical channel, the right column the horizontal channel. The upper section of each panel shows the phase, the lower section the amplitude. The slope in the phase results from the delay of each antenna w.r.t. the reference, ea06. The notches in the amplitude gains are due to the anti-aliasing function of the WIDAR correlator. **Right Panel:** Showing the cross-hand phase solutions, using DA240 as the calibrator source. A 85 degree slope, due to the cross-hand delay, has been removed via application of `RLDLY`.

180 degrees, are possible, and imaging of the highly polarized calibration source is needed to determine which is the correct value[12]. `VHDIF` includes a `DOINVERS` adverb, which adds 180 degrees to the solutions. We refer the reader to Section 5.3 of EVLA Memo #207 for details. The resulting (correct) cross-hand phase is shown in the right-hand panel of Fig. 1.

We emphasize that the use of a single observation to perform the amplitude and phase balancing requires the signal transmission system having good gain stability over the length of an observation. In fact, the VLA's amplitude and phase gains are usually very stable over time. Significant variations in the V-to-H gain ratios over time can be corrected by utilizing multiple observations of a strong, unpolarized source[13].

At this point, the linear-basis data are sufficiently balanced in amplitude and phase to enable accurate conversion to a circular basis. This was done by utilizing the new *AIPS* program `VH2RL`. Following this, the standard calibration routine for a circular-basis dataset was followed:

1. `FRING`. The delay solutions are all very small – of order 0.1 nsec – since the `BPASS`, `RLDLY`, and `VHDIF` operations, used to balance the linear gains, have already removed all delays. The phase solutions, for four antennas, are shown in the left-hand panel of Fig. 2. These phase solutions show significant temporal variations, since the phase solutions in the linear-basis data were made from a single bandpass observation. The phase fluctuations increase with increasing baseline, as expected from P-band observations in C-configuration due to ionospheric irregularities.

2. `BPASS`. The solutions are near unity amplitude (deviations less than 0.5%) and zero phase (deviations less than 0.5 degrees), as the spectral variations were removed in the linear-basis amplitude and phase balancing.

3. `CALIB`. All four calibrator sources can now be included for detailed gain solutions, as their linear polarizations will not affect the parallel-hand gains. The resulting gains – following determination of their spectral flux densities– are shown in the right-hand panel of Fig. 2 for these four antennas. The values are not near unity, as a 1-Jy flux was assumed in the linear `BPASS` calibration[14].

4. `RLDLY`. This step removes the cross-hand delay between the R and L channels. The observed delay is less than 0.5 nsec, as the cross-hand delays were removed in the linear calibrations.

[12]Application of the wrong solution will generally result in no visible polarized emission.

[13]Note that poor atmospheric phase stability is not a problem at this stage, since these fluctuations are the same in both polarization channels.

[14]Since these solutions are in voltage units, the source flux density is equal to the square of the values – ∼53 Jy.

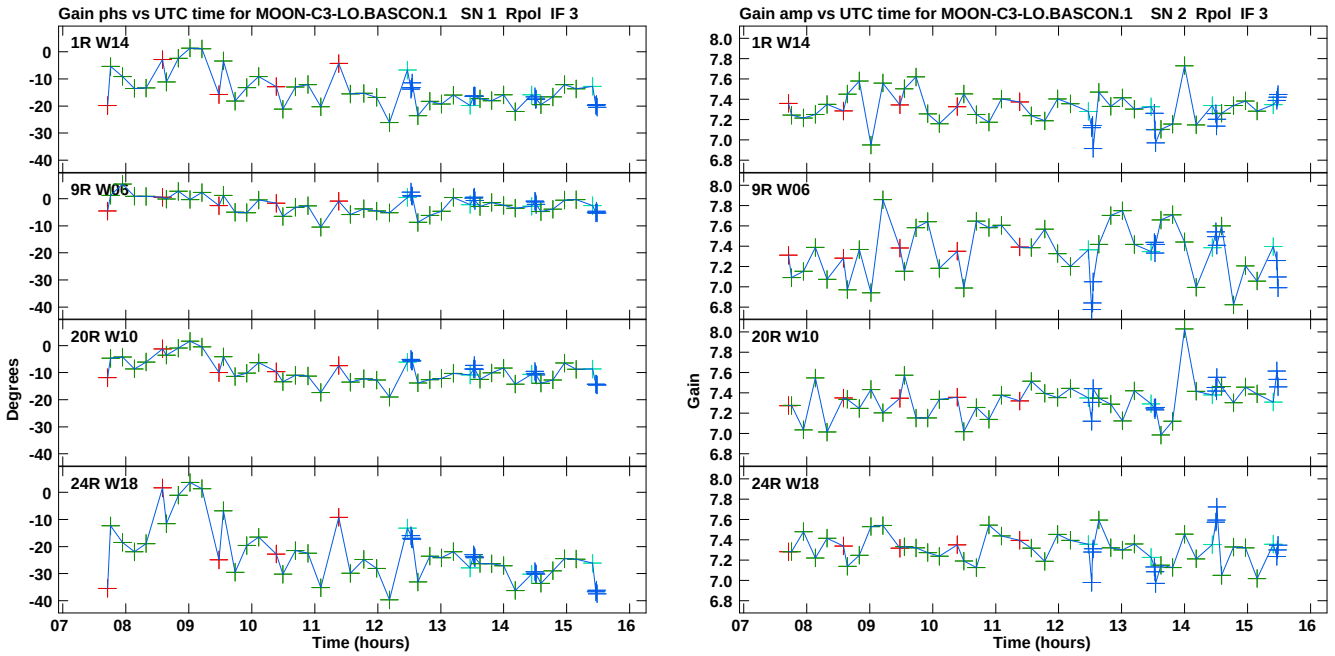

Figure 2: **Left Panel:** Showing the R phase gain solutions for four antennas, using all four calibration sources. Note the phase stability significantly worsens with baseline length. The sources are color-coded: Red shows 3C147, blue for 3C295, green for the lunar calibrator J1021+2159. The second observation of 3C147 shows zero phase, as it was this scan used to calibrate the bandpasses in the linear-based data. **Right Panel:** Showing the amplitude gain solutions from the four calibration sources. Most of the scatter is due to the low flux density of the gain calibrator J1021+2159.

5. `PCAL`. This solves for the cross-hand leakages. For low frequency applications, it is necessary to use unpolarized sources, as the program cannot separate a time-varying (due to ionospheric Faraday rotation) astronomical polarized signal from a time-invariant receiver leakage[15]. We used 3C147 and 3C295 for this example. Because the linear feeds provide quite high polarization purity, we expect the resulting circularly converted data to also show high purity. Examples for three antennas are shown in the left-hand panel of Fig. 3, which are indeed quite low – typically 2%.

6. `TECOR`. The observed position angles for polarized emission at these low frequencies can be greatly rotated by Faraday rotation in the ionosphere. For circular-basis data, these rotations show up as phase offsets in the cross-hand correlations. It is important that the cross-hand correlations take account of these rotations prior to the use of any cross-hand (RL and LR correlators) data. This program calculates and applies these phases.

7. `RLDIF`. This program adjusts the R-L phase to obtain the correct alignment of the EVPA. This operation requires knowledge of the EVPA, as a function of frequency, of one strongly polarized source. We used DA240, for which the source RM is known to be 3.22 rad/m^2, and whose intrinsic (zero-wavelength) EVPA is -114 degrees[16]. The resulting phase solutions are shown in the right-hand panel of Fig. 3.

In the preceding description, it will be noted that the `FRING`, `BPASS`, and `RLDLY` functions all returned unit amplitude and zero phase values – a result of the preceding gain balancing of the linear-basis data. Hence executing the programs was not actually needed here. Indeed, had we utilized the known flux of 3C147 in the linear-basis calibration, and solved for gain as a function of time using that source, the `CALIB` operation in the circular-basis calibration would also have been superfluous. Presuming good initial gain calibration of the linear-basis data, only the `PCAL`, `TECOR`, and `RLDIF` operations are needed in the circular-basis data[17].

Imaging results from these procedures will be shown in a following memo.

[15] In the absence of ionospheric rotations, the program can solve for the astronomical source polarizations and the instrumental polarizations, provided the observations span a sufficient range in parallactic angle.

[16] Refer to the following EVLA Memo for the derivation of these values.

[17] Note, however, that if it is desired to utilize a known linearly-polarized calibrator in the gain calibration process of the linear-basis data, `CALIB` will need to be run.

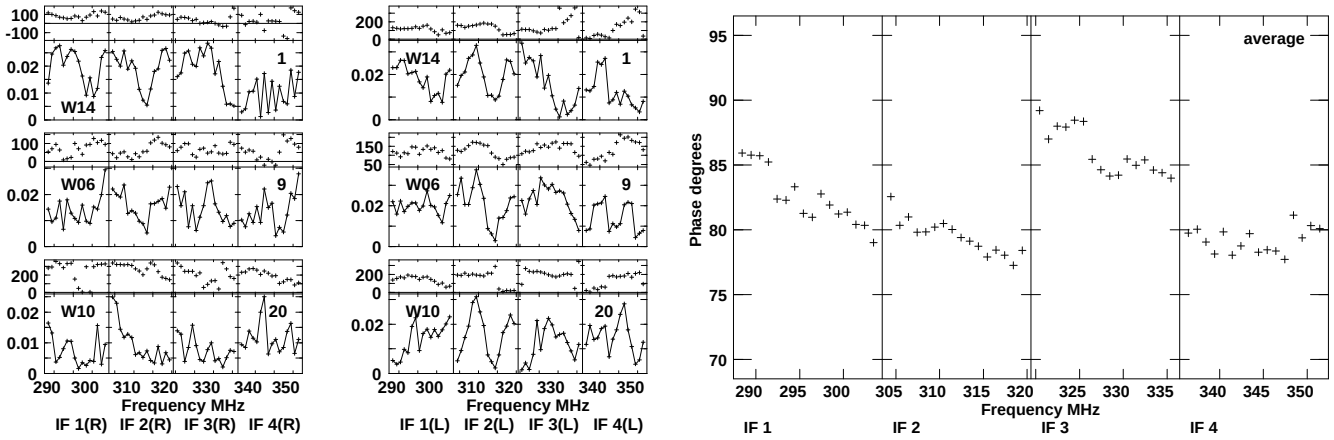

Figure 3: **Left Panel:** Showing the cross-polarization solutions for three typical antennas, with RCP on the left, LCP on the right. In each of the six panels, the phase solutions are on top, amplitude solutions below. All amplitude values are small – typically 2%. **Right Panel:** Showing the cross-hand phases required to align the source polarization position angles.

4.2 MeerKAT Data Example

The MeerKAT array's UHF-band utilizes a low-frequency, linearly-polarized receiver system covering ∼540 – 1100 MHz. We have utilized a lunar observation taken with this array on 22Jun2021 to test our conversion routines. Unlike the VLA's P-band system, the MeerKAT UHF receivers have an on-board calibration system which removes nearly all the cross-hand delay. This simplifies the processing needed for conversion to a circular basis.

These MeerKAT data are much less affected by RFI than the VLA's P-band system, so we show here the entire bandwidth, spanning 544 through 1088 MHz. The MeerKAT correlator provides the data in a single 'spectral window'. As *AIPS* expects data broken into multiple spectral windows, we converted the data to a 16-SPW dataset, with each SPW spanning 34 MHz. Following essential flagging, the data were decimated to 24 second averaging, and 2.125 MHz channel width for faster processing.

The `BPASS` operation was done on a single scan of J1939-6342, an unpolarized and unresolved standard flux calibrator. The flux density was known in advance, and was utilized for the solutions. The resulting bandpasses, for three selected antennas, are shown in the left-hand panel of Fig. 4. As the cross-hand delays in these data had

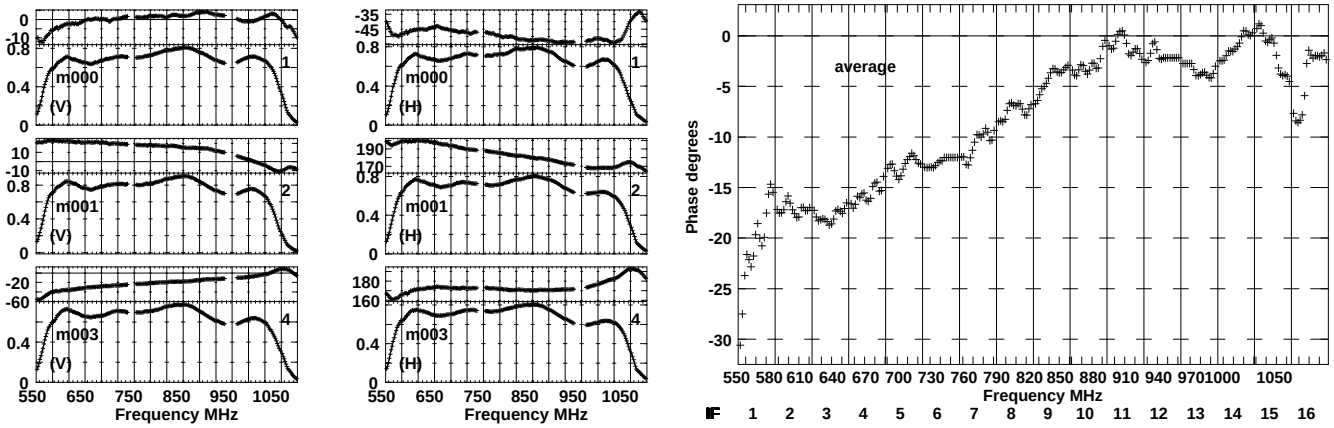

Figure 4: **Left Panel:** Showing the absolute bandpass solutions from J1939-6342, for antennas m000, m001, and m003. The left column shows the vertical channel, the right column the horizontal channel. The upper section of each panel shows the phase, the lower section the amplitude. The slope in the phase results from the delay of each antenna w.r.t. the reference, m002. **Right Panel:** Showing the cross-hand phase solutions, using 3C286 as the calibrator source. There is only a small residual cross-hand delay in these data.

already been removed by the on-line system, the `RLDLY` program, needed for the VLA data, was not required. We

thus went straight to the VHDIF operation, utilizing 3C286, to remove any residual cross-hand phase. The results are shown in the right-hand panel of Fig. 4.

The data were then transformed to a circular basis via VH2RL, and the standard circular calibration procedures performed. As with the VLA data, the FRING and BPASS operations provided close to zero phase and unit amplitude corrections. Because the gain normalization operation (BPASS) in the linear dataset utilized the known flux density of the calibrator, the CALIB operation on the circulars provided near unit amplitude solutions as well. Examples of the phase and amplitude solutions are shown in Fig. 5. The notable phase offsets for 3C286 and J1939-6342 are

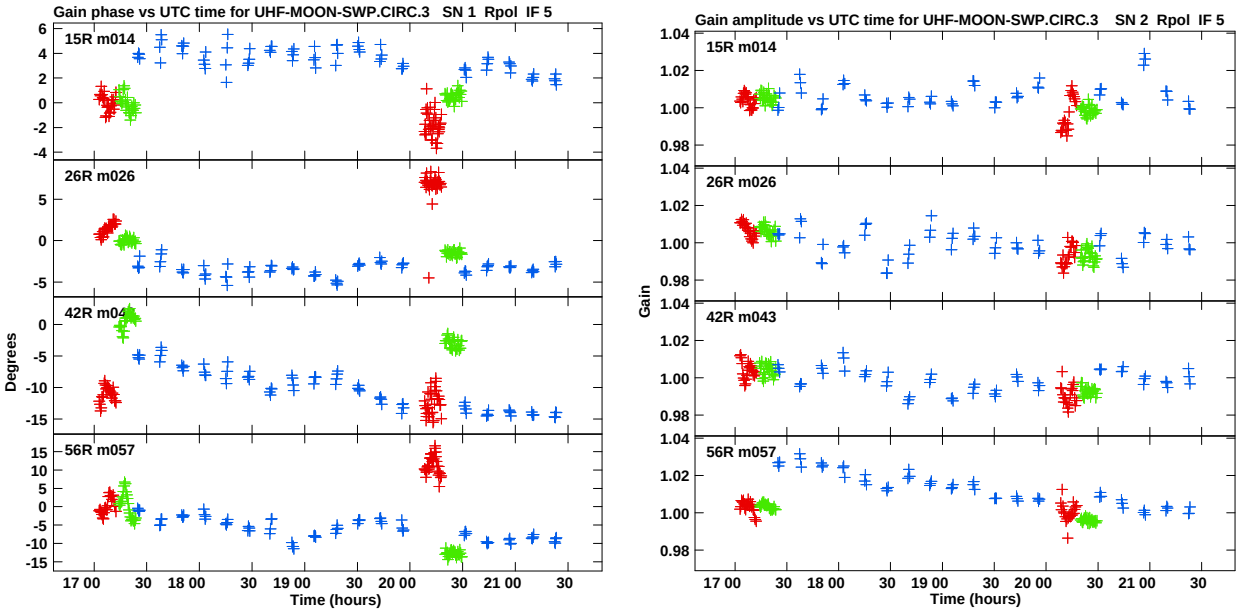

Figure 5: **Left Panel:** Showing the phase gain solutions for four antennas, using all three calibration sources. The sources are color-coded: Red shows 3C286, blue for the nearby lunar calibrator J1733-1304, and green for the flux calibrator J1939-6342. The first observation of J1939-6342 shows zero phase, as it was this scan used to calibrate the bandpasses in the linear-based data. **Right Panel:** Showing the amplitude gain solutions from the three calibration sources. The values are near unity, as the known flux density of J1939-6342 was used in the gain normalization process.

likely due to incorrect baseline coordinates – these sources are both at very different declinations than the moon and its nearby calibrator. The RLDLY operation was performed next – a small delay of 0.31 nsec was removed from the data. Following this, PCAL was run, and the results are shown in the left-hand panel of Fig. 6. It will be noted that the cross-polarizations in these MeerKAT data are considerably smaller than those on the VLA data. This is true for nearly all the MeerKAT antennas, which appear to have been designed to prevent significant coupling between the polarized channels.

The final operation was running RLDIF, using the known polarized calibrator 3C286. The required R-L phase solutions are shown in the right-hand panel of Fig. 6. Examples of the resulting images will be shown in a following memo.

5 Inclusion of Antenna Cross-Polarization

We have noted earlier the requirement that the linearly-polarized data be accurately amplitude and phase balanced prior to conversion to a circular basis. Here we discuss the preferred accuracy.

Sadly, antennas are not purely polarized. Inevitably, some of the signal in one polarization channel couples into the other channel. In terms of the antenna's ellipticity, there is a small deviation from the pure state. Thus, for a linearly-polarized antenna, the antenna ellipticity has a small value $\chi \ll 1$, while for a circularly-polarized antenna, the ellipticity is slightly less (in absolute value) than $\pi/4$.

In the standard treatments (e.g. Thompson, Moran, and Swenson), these leakage signals are quantified by D

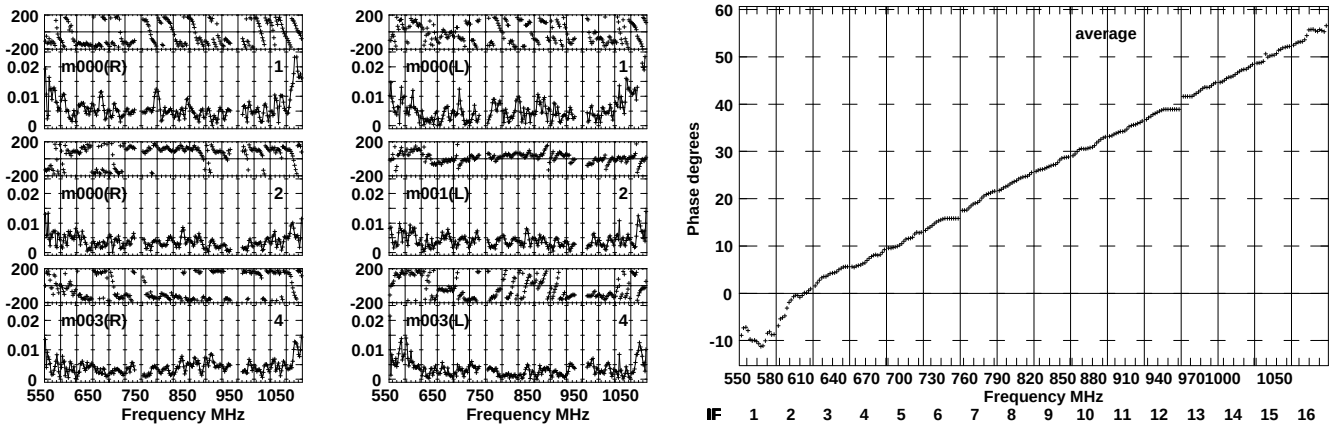

Figure 6: **Left Panel:** Showing the cross-polarization solutions for three typical antennas, with RCP on the left, LCP on the right. In each of the six panels, the phase solutions are above, amplitude solutions below. All amplitude values are very small – typically 0.5%. **Right Panel:** Showing the cross-hand phases required to align the source polarization position angles, using the polarized calibrator 3C286. Because these data were taken at low frequency, the Faraday rotation correction program TECOR was run before `RLDIF`.

terms[18]. So, for example, they write, for the relation between the observed visibility, V^{obs}, and the true visibility, V:

$$\begin{pmatrix} V_v^{obs} \\ V_h^{obs} \end{pmatrix} = \begin{pmatrix} 1 & D_{hv} \\ D_{vh} & 1 \end{pmatrix} \begin{pmatrix} V_v \\ V_h \end{pmatrix} \tag{21}$$

where the 2 x 2 Jones matrix describes the leakage of signals from one polarization channel to the other. Again forming the outer product operation, we obtain the relations between the observed correlated products, and the true products:

$$\begin{pmatrix} R_{vv}^{obs} \\ R_{vh}^{obs} \\ R_{hv}^{obs} \\ R_{vv}^{obs} \end{pmatrix} = \begin{pmatrix} 1 & D_{hv2}^* & D_{hv1} & D_{hv1}D_{hv2}^* \\ D_{vh2}^* & 1 & D_{vh1}D_{vh2}^* & D_{hv1} \\ D_{vh1} & D_{vh1}D_{hv2}^* & 1 & D_{hv2}^* \\ D_{vh1}D_{vh2}^* & D_{vh1} & D_{vh2}^* & 1 \end{pmatrix} \begin{pmatrix} R_{vv} \\ R_{vh} \\ R_{hv} \\ R_{hh} \end{pmatrix} \tag{22}$$

The leakages in the linear-basis correlations R_l will show up as D term leakages in the circular converted correlations R_c. In general, analysis shows that the amplitudes of the resulting circular D terms will be similar to those in the originating linear D terms. Thus, the $\sim 2\%$ amplitudes of these terms shown in the preceding section in VLA data are thus believed to reflect the purity of the linear systems.

There is one special exception to the preceding statements – the leakages in the linear basis data due to differential antenna rotation. This may be caused by mis-orientation of the linear feed dipoles, or by differential parallactic angles. This situation is worthy of a more detailed analysis. Presume an antenna's orthonal feeds or receiver are misoriented by an angle θ with respect to the reference direction. For the linear-basis Jones matrix, we then write for the observed output voltages

$$\begin{pmatrix} V_v^{obs} \\ V_h^{obs} \end{pmatrix} = \begin{pmatrix} \cos\theta & \sin\theta \\ -\sin\theta & \cos\theta \end{pmatrix} \begin{pmatrix} V_v \\ V_h \end{pmatrix} \tag{23}$$

Comparison to Equation 21 shows that the D terms are real, with leakage amplitude equal to $\sin\theta$ which, for the usual situation where the misorientations are small, is approximately equal to θ. A CCW misalignment gives a positive D term, a CW misalignment a negative term[19].

For the circular case, Equation 21 after insertion into the defining conversion matrix (Equation 18), and forming the circular products, produces a very different relation:

$$\begin{pmatrix} V_r^{obs} \\ V_l^{obs} \end{pmatrix} = \begin{pmatrix} e^{-i2\theta} & 0 \\ 0 & e^{i2\theta} \end{pmatrix} \begin{pmatrix} V_r \\ V_l \end{pmatrix} \tag{24}$$

[18]Analysis shows that these terms are related to the antenna ellipticity and position angles by: $D_r = \tan\beta_r e^{i2\phi_r}$, and $D_l = \tan\beta_l e^{-i2\phi_l}$, where $\beta_r = \pi/4 + \chi_r$, and $\beta_l = \pi/4 - \chi_l$, and ψ_r and ψ_l are the antenna ellipse major axis orientations, referenced to the antenna frame.

[19]A more careful analysis takes into account the $\cos\theta$ loss term in the matrix, which after gain calibration results in the D term amplitudes being given by $\tan\theta$, which in the small-angle limit gives the same result cited above.

– the off-diagnonal D terms are all zero! This special case of misaligned dipoles transforms the rotation into phase offsets in the parallel hand voltages in the circular basis[20]. This result illustrates a great advantage of the circular-basis system – all rotations, including receiver misalighments, parallactic angle orientations, and ionospheric rotations, transform to phase rotations in the data, leaving the correlation amplitudes unchanged.

We illustrate these points in Figure 7. Here we show the calculated D terms for two VLA antennas with the original linear-basis data (left panel) and the corresponding terms when the data are converted to a circular basis (right panel). The two antennas are chosen to illustrate the effect of a large positive rotation (ea03, in the upper panels), and a large negative rotation (ea07, in the lower panels), with respect to the reference antenna, ea06. According to the preceding analysis, antenna rotation – relative to the orientation of the reference antenna – is manifested in the linear system by a real D-term whose amplitude is given by $\sin\theta \sim \theta$, while in the circular system, it shows up as a phase term in the parallel-hand gains, which is accounted for the the gain calibration process.

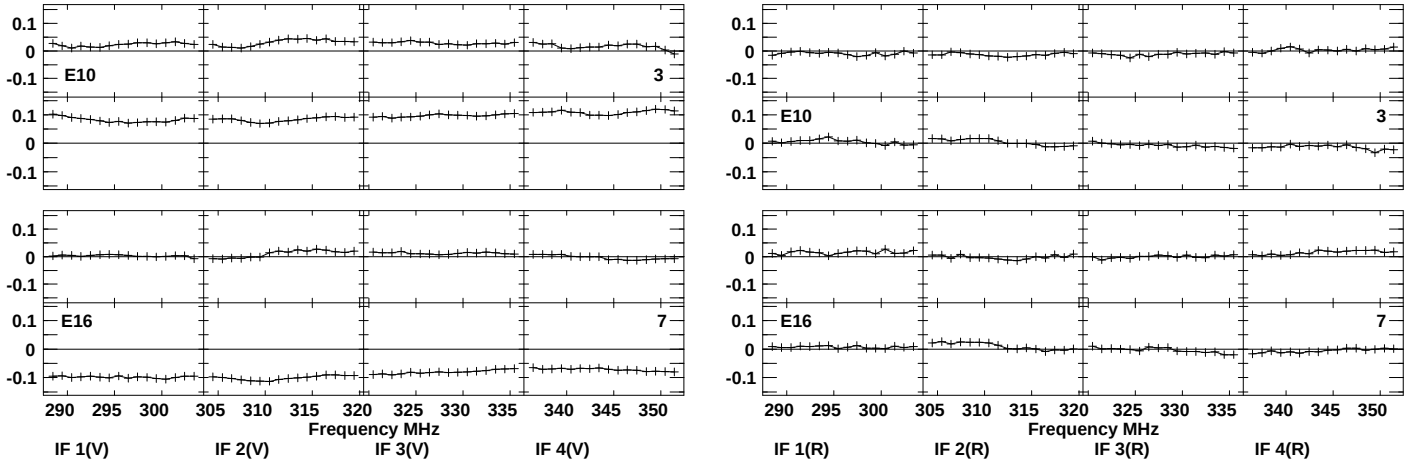

Figure 7: The calculated cross-polarizations (D terms) for two VLA antennas with significant dipole misorientations w.r.t. the reference, for the originating linear-basis data, and the converted circular-basis data. **Left Panel:** Ea03 (top) and ea07 (bottom) for the linear-basis. For each, the imaginary part is plotted on top, the real part below. Note the imaginary parts for both antennas are very small, typically 2%, while the real parts are large, typically 10%, and constant in frequency, as expected for a rotation. **Right Panel:** The corresponding D-terms when the data are transformed to the circular basis, for the R polarization. All values are now small, less than $\sim 2\%$.

In Fig. 7, each of the four panels shows the imaginary (top) and real (bottom) values of the complex D leakage terms. The two left panels show the leakages for the V polarization for antenna ea03 (above) and ea07 (below). The two right panels show the corresponding leakages for these antennas after conversion to circular. The linear-based terms show small imaginary, but large real components, reflecting their origin as misorientations of the antenna dipoles. The values of +0.1 and -0.1 suggest rotations of about +6 and -6 degrees, respectively. This interpretation is not unique – the coupling could be due to processes further down the signal chain. However, the fact that the real parts are nearly constant over the full frequency range, and that the values for the H polarization (not shown) are of the same amplitude and of opposite sign, provide very strong evidence in favor of the cause being due to dipole misorientation[21].

The right-hand panels show, on the same scale, the corresponding D terms in the circular system for the converted R polarization. All values are very small – typically $\sim$1%, showing that the circularly-converted data are very nearly pure . The effects of the antenna mis-orientations are moved to the phases, and have been removed from the parallel-hand correlations as part of the regular gain calibration. Indeed, the cross-polarization terms are now so small that it may suffice to not calculate them at all for reasonable polarimetry.

We noted in the last section that the MeerKAT UHF-band linear and circular-converted data show much smaller cross-polarizations than the VLA P-band data. Both the distribution in rotations among the MeerKAT antennas is smaller, and the residual circular D-terms are smaller than those in the VLA's P-band data. Examples of this are shown in Fig. 8 for the MeerKAT data. Note that the amplitude scales are a factor of six smaller than the

[20]This is easy to understand: Rotating a circularly polarized antenna changes the phase of a circularly polarized signal, but not the amplitude.

[21]Plus the fact that visual observation of these feeds show misorientations of a few degrees are common!

corresponding values for the VLA.

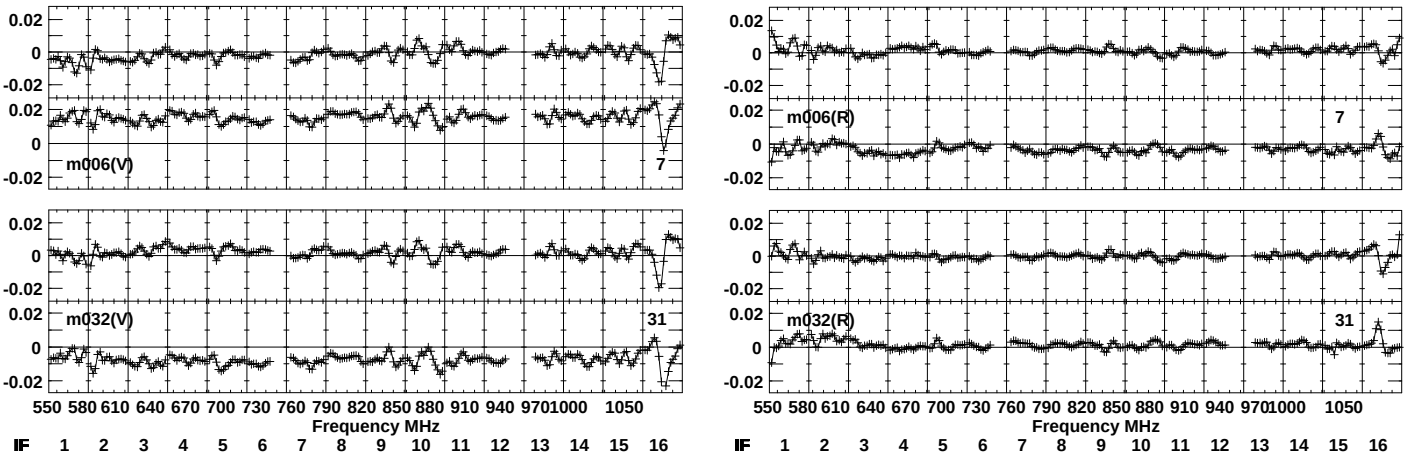

Figure 8: The calculated cross-polarizations (D terms) for two MeerKAT antennas (m008, top, and m032, bottom) with significant dipole misorientations w.r.t. the reference, in the linear and circular bases. For all panels, the imaginary part is plotted on top, the real part below. **Left Panel:** The V cross-polarization for the linear basis. Note the imaginary parts for both antennas are very small, typically 0.05%, while the real parts are larger, typically 2%, and constant in frequency, as expected for a rotation.**Right Panel:** The same antennas as seen in a circular basis, for the R polarization. All values are now very small, less than $\sim 0.05\%$.

The $\sim$0.02 value for the imaginary component in the figure for m007 informs us that a feed rotation of $\sim$ 1 degree is present – this is the largest value we could find in the solutions. The spread in the MeerKAT antenna feed orientations is much smaller than that for the VLA! Examination of the right panel shows that the typical values for both real and imaginary parts of the circular D-terms is nearly negligible – less than 0.005 for nearly all channels. This is so good that it seems likely that antenna polarization calibration is hardly needed at all!

6 Summary

If, as we believe, wide-band receivers providing linear-basis signals are more sensitive, and of higher polarization purity than those after conversion to a circular basis by an antenna-based imperfect analog device, it is clearly preferable to utilize linear-basis data for astronomical observations. However, there are significant complications in gain calibration of these linear-basis signals, both in regular gain calibration, and in self-calibration of polarized target sources. The basic complications in utilizing linear-basis data directly for calibration arise from the need to know the polarization state of the calibrators. Not only is this not known in advance for the more than 1000 calibrators, but this state is variable on timescales of days to years for nearly all the commonly-used calibrators. Further complicating this at low frequencies are the highly variable (seconds to hours) rotations induced by Faraday rotation in the Earth's ionosphere.

All these complications can be bypassed by utilizing data in a circular basis, as the linear-polarization information is solely located in the cross-hand correlations. All calibration operations utilizing the high-signal parallel-hand data can then proceed without concern for source polarization characteristics. These advantages also apply to the vital process of self-calibration of target sources.

We have shown in this memo how the nearly-pure linear-based data can be easily transformed to equally pure circular-based data, following straightforward amplitude and phase balancing. The resulting circular-based data then enable superior calibration, utilizing all potential calibration sources, without regard to their unknown polarization states, and imaging. A new *AIPS* task `VH2RL` generates the converted data, which we have tested with VLA P-band, and MeerKAT UHF-band data. Results from these, and other, datasets will be reported in an upcoming memo.

7 Acknowledgements

We thank Oleg Smirnov and Wes Grammar for useful comments and corrections.